Polyampholytic Hydrogel Swelling Transitions: Limitations of the Debye−Hückel Law

Anthony E. English*

Harvard-MIT Division of Health Sciences and Technology, Massachusetts Institute of Technology, Cambridge, Massachusetts 02139

Toyoichi Tanaka

Department of Physics and Center for Materials Science and Engineering, Massachusetts Institute of Technology, Cambridge, Massachusetts 02139

Elazer R. Edelman

Department of Internal Medicine, Cardiovascular Division, Brigham and Women's Hospital and Harvard Medical School, Boston, Massachusetts 02115, and Harvard-MIT Division of Health Sciences and Technology, Massachusetts Institute of Technology, Cambridge, Massachusetts 02139

Received August 8, 1997; Revised Manuscript Received December 23, 1997

ABSTRACT: This study has examined polyampholytic hydrogel swelling transitions over a wide range of bath salt concentrations. Copolymer 2-acrylamido-2-methyl-1-propanesulfonic acid (AMPS−H) and [3-(methacryloylamino)propyl] trimethylammonium chloride (MAPTA−C1) hydrogels were prepared with a total monomer concentration of 1.4 M near the charge balance point. Hydrogel equilibrium swelling measurements were made in aqueous baths having sodium chloride concentrations ranging from 1 μM to 1 M. The observed swelling transitions have been interpreted using a series of thermodynamic models based on successively higher order Mayer ionic solution theory corrections. Collapse transitions at low and intermediate bath salt concentrations observed experimentally were successfully predicted using only a zero order Mayer, or Donnan model, approximation. First order Mayer corrections, equivalent to the Debye−Hückel limiting law (DHLL), failed to produce physically meaningful results at the polymer ion and bath salt concentrations of interest in this study. However, a second order Mayer correction, equivalent to the Debye−Hückel limiting law + second virial coefficient (DHLL + B_2), was in qualitative agreement with our experimental results. Further improvements based on the straightforward extension to higher order Mayer approximations are discussed.

Introduction

Polyampholytic hydrogels consist of positive, negative, and even neutral monomeric species that are polymerized and cross-linked into a three-dimensional network. Most potential applications of polyampholytes concern their porosity or swelling behavior when immersed in high-concentration electrolyte baths.[1−3] Unlike polyelectrolytes, polyampholytes have the unique capacity to swell and remain soluble at high ionic strengths. This property has a number of important implications for their technological use. In particular, a number of potential medical applications require a quantitative understanding of these materials at physiologic ion strengths. Recent experimental studies have shown that, depending on the magnitude of the net polymer charge and bath ionic strength, the swelling properties can be dominated by acid and base dissociation, electrostatic repulsion, and electrostatic attraction.[4,5]

Polyampholytes have been the subject of many theoretical studies since they provide a model for studying the long-range interactions found in proteins and other forms of soft condensed matter.[6−10] Most theoretical treatments of polyampholyte swelling, however, have been based on the Debye−Hückel limiting law (DHLL) osmotic correction, which is only valid at low ion concentrations.[1,11,12] The electrostatic interactions between polymeric and mobile charges that determine the hydrogel swelling equilibrium at high ionic strengths are, therefore, still not very well understood.

The foundations for a quantitative description of osmotic pressure, analogous to the virial expansion for nonideal gases, were established in a landmark paper by McMillan and Mayer.[13] Mayer later extended the McMillan−Mayer model to include the long-range Coulombic and short-range hard core molecular interactions characteristic of ionic solutions.[14] The numerical solutions to liquid state integral equations and their relation to the Mayer ionic solution theory have also proved invaluable in the study of ionic solutions at high concentrations.[15−18] Few studies, however, have examined ionic contributions to polyampholyte swelling beyond the DHLL in systems where a hydrogel phase exists in equilibrium with a bath phase.

The objective of this study is to examine polyampholytic hydrogel swelling transitions over a wide range of bath salt concentrations. Copolymer 2-acrylamido-2-methyl-1-propanesulfonic acid (AMPS−H) and [3-(methacryloylamino)propyl]trimethylammonium chloride hydrogels prepared with a total monomer concentration of 1.4 M near the charge balance point are investigated. Hydrogel swelling equilibrium measurements are made in aqueous baths having sodium chloride concentrations ranging from 1 μM to 1 M. These swelling measurements are then interpreted using a series of thermodynamic models based on

* Author to whom correspondence should be addressed. Telephone: (617) 252-1655.

S0024-9297(97)01207-2 CCC: $15.00
Published on Web 02/27/1998

successively higher order Mayer ionic solution theory corrections. The necessary level of approximation required to predict the various swelling transitions is discussed.

Experimental Section

Copolymer hydrogels with varying proportions of AMPS−H and MAPTA−Cl were fabricated. To estimate the charged monomer balance point and remove impurities from the pregel solution, a counterion precipitation technique using the silver salt of AMPS−H was used. The AMPS-MAPTA polyampholyte pregel solution was prepared by initially making a 1.0 M aqueous solution of AMPS−H at approximately 4 °C. While stirring the AMPS−H solution, Ag_2CO_3 was slowly added to produce an equivalent concentration of 1.0 M AMPS−Ag. The solution was then centrifuged at 3000 rpm and filtered with a 0.2 μm filter. After MAPTA−Cl was added, the resulting AgCl precipitate was filtered out using a 0.2 μm filter. Small aliquots of the AMPS−MAPTA solution were tested with MAPTA−Cl and AMPS−Ag to ensure the solution had an approximately equal concentration of AMPS and MAPTA monomers.

The hydrogels were cross-linked using 8.6 mM *N,N′*-methylene-bis-acrylamide (BIS). Polymerization was initiated using 1.76 mM ammonium persulfate (APS), and the gelation temperature was 60 °C. Hydrogel samples with a net charge offset were made by adding AMPS−Na, while the total monomer concentration was kept at 1.4 M. The AMPS−Na solution used to offset the balanced pregel solution was produced by neutralizing AMPS−H with an equal molar concentration of NaOH. The hydrogels were cast in 200 μm inner diameter micropipets. After the hydrogels were continuously washed for several days, diameter measurements were made using a microscope equipped with a video camera.

Theoretical Background

System Free Energy. The system free energy can be considered a sum of elastic, solvent, and ionic components. The ionic contribution to the hydrogel swelling equilibrium can be represented as a series of approximations that include more terms of a Mayer ionic solution virial expansion. The zero order contribution from the Mayer expansion is equivalent to the Donnan approximation and includes only the mobile ion translational entropy. Adding first order corrections gives rise to the DHLL, while including terms up to second order is equivalent to the Debye−Hückel limiting law + second virial coefficient (DHLL + B_2). Other methods that include specific types of terms in the Mayer expansion, such as the Percus−Yevick (PY) and hypernetted chain (HNC) approximations, can also be considered.

The total system free energy, ΔF^{T}, can be decomposed into a sum of hydrogel and bath components such that

$$\Delta F^{\mathrm{T}} = \Delta F^{\mathrm{H}} + \Delta F^{\mathrm{B}} \tag{1}$$

where ΔF^{H} and ΔF^{B} represent the hydrogel and bath contributions, respectively. The hydrogel free energy can be written as

$$\Delta F^{\mathrm{H}} = \Delta F_{\mathrm{M}} + \Delta F_{\mathrm{el}} + \Delta F_0 + \Delta F_{\mathrm{ex}} \tag{2}$$

where ΔF_{M} and ΔF_{el} represent the solvent and elastic contributions. The term ΔF_0 represents the zero order translational component of the mobile ions and ΔF_{ex} the excess free energy correction.

As described in previous studies,[4,5,19] the solvent and elastic contributions to the free energy are given by the relations

$$\Delta F_{\mathrm{M}} = k_{\mathrm{B}}T\frac{V}{v_{\mathrm{site}}}(1-\phi)[\ln(1-\phi)+\chi\phi] \tag{3}$$

$$\Delta F_{\mathrm{el}} = \frac{3k_{\mathrm{B}}T}{2}\frac{V\phi}{N_{\mathrm{x}}v_{\mathrm{site}}}\left[\left(\frac{\phi_0}{\phi}\right)^{2/3} - 1 - \frac{1}{3}\ln\left(\frac{\phi_0}{\phi}\right)\right] \tag{4}$$

where k_{B} is the Boltzmann constant, T the absolute temperature, V the hydrogel volume, v_{site} the lattice site volume, ϕ the polymer volume fraction, and ϕ_0 the polymer volume fraction in the reference or initial state. The polymer and solvent interaction parameter is represented by χ and N_{x} is the number of monomers between cross-links.

The translational freedom of the ions within the hydrogel make a zero order contribution of the form

$$\Delta F_0 = k_{\mathrm{B}}T\sum_{i=1}^{\sigma}N_{\mathrm{i}}\left\{\ln\left(\frac{N_i}{V}\right) - 1\right\} + \sum_{i=1}^{\sigma}z_{\mathrm{i}}eN_{\mathrm{i}}\varphi \tag{5}$$

where z_i is the ith ion valance, N_i is the number of ith particles in the hydrogel phase, e is the unit electrostatic charge, and σ is the number of ion species. The term φ represents the uniform contribution to the internal potential energy arising from the electrostatic double layer at the hydrogel boundary.[19]

The first order correction to the excess free energy is given by the DHLL,[20,21]

$$(\Delta F_{\mathrm{ex}})_{\mathrm{DHLL}} = -k_{\mathrm{B}}TV\frac{\kappa^3}{12\pi} \tag{6}$$

where the inverse Debye length, κ, is defined as

$$\kappa = \left[\frac{\sum_{i=1}^{\sigma}c_i{z_i}^2e^2}{\epsilon\epsilon_0k_{\mathrm{B}}T}\right]^{1/2} \tag{7}$$

for a medium having a dielectric constant ϵ and where ϵ_0 is the permittivity of free space. In the extended Debye−Hückel limiting law[21] the free energy is defined as

$$(\Delta F_{\mathrm{ex}})_{\mathrm{DHLL'}} = -k_{\mathrm{B}}TV\frac{\kappa^3}{12\pi}\tau(\kappa\alpha) \tag{8}$$

where

$$\tau(\kappa a) = \frac{3}{\kappa^3a^3}\left\{\ln(1+\kappa a) - \kappa a + \frac{\kappa^2a^2}{2}\right\} \tag{9}$$

is an excluded volume correction for ions with a hard core radius of a.

Including second order virial expansion corrections in the Mayer ionic solution theory for ΔF_{ex} gives us the DHLL + B_2 approximation,[22]

$$(\Delta F_{\mathrm{ex}})_{\mathrm{DHLL+B_2}} = -k_{\mathrm{B}}TV\left(\frac{\kappa^3}{12\pi} + \sum_{i=1}^{\sigma}\sum_{j=1}^{\sigma}c_ic_jB_{ij}(\kappa)\right) \tag{10}$$

where c_i is the concentration of the ith ion and B_{ij} is

the second virial coefficient given by

$$B_{ij}(\kappa) = 2\pi\int_0^\infty \left\{\exp\left[-\frac{u^*_{ij}(r)}{k_B T}\right]\exp(q_{ij}(r)) - 1 - q_{ij}(r) - q_{ij}^2(r)/2\right\} r^2\, dr \quad (11)$$

The short-range potential, $u^*_{ij}(r)$, is typically modeled as a hard sphere interaction, and

$$q_{ij}(r) = -\left(\frac{z_i z_j e^2}{4\pi\epsilon\epsilon_0 k_B T r}\right)\exp(-\kappa r) \quad (12)$$

is the screened Coulomb interaction potential for a pair of ions i and j separated by a distance r.

Equation 10 is equivalent to the simpler expression

$$(\Delta F_{ex})_{DHLL+B_2} = -k_B T V\left(\frac{5\kappa^3}{96\pi} + \sum_{i=1}^{\sigma}\sum_{j=1}^{\sigma} c_i c_j S_{ij}(\kappa)\right) \quad (13)$$

where

$$S_{ij}(\kappa) = 2\pi\int_0^\infty \left\{\exp\left[-\frac{u^*_{ij}(r)}{k_B T}\right]\exp(q_{ij}(r)) - 1\right\} r^2\, dr \quad (14)$$

Higher order corrections to the free energy beyond the DHLL + B_2 approximation can be found by first evaluating the radial distribution functions, $g_{ij}(r)$, for each particle species pair using integral equation methods. Much interest has been given to calculating the radial distribution functions from the hypernetted chain (HNC) and Percus−Yevick (PY) equations.[16−18] The contribution to the excess osmotic pressure from the radial distribution functions is

$$\pi_{ex} = -\frac{1}{6}\sum_{i=1}^{\sigma}\sum_{j=1}^{\sigma} c_i c_j \int_0^\infty r\,\frac{\partial u_{ij}(r)}{\partial r}\, g_{ij}(r)(4\pi r^2)\, dr \quad (15)$$

where $u_{ij}(r)$ is the radially dependent potential energy between particles i and j. The corresponding contribution to the free energy is

$$\Delta F_{ex} = \int_0^c \pi_{ex}\, d\ln c' \quad (16)$$

where

$$c = \sum_{i=1}^{\sigma} c_i \quad (17)$$

and c' is an integration variable also representing the total concentration of particles.

Similar corrections to the free energy of the surrounding bath can be made by modeling the total bath free energy as a sum of zero order and excess free energy contributions such that

$$\Delta F^B = \Delta F_0^B + \Delta F_{ex}^B \quad (18)$$

where

$$\Delta F_0^B = k_B T\sum_{i=1}^{\sigma} N_i^B\left\{\ln\left(\frac{N_i^B}{V^B}\right) - 1\right\} + \sum_{i=1}^{\sigma} z_i e N_i^B \varphi^B \quad (19)$$

and ΔF_{ex}^B is the excess free energy of the bath phase. In eq 19 N_i^B is the number of ith particles in the bath phase, V^B is the volume of the bath phase, and φ^B is the uniform potential component in the bath phase.

Thermodynamic Equilibrium. In equilibrium the chemical potentials of both the solvent and mobile ion species in the hydrogel and bath phase balance. Balancing the solvent chemical potentials, for example, is equivalent to balancing the osmotic pressures according to the relation

$$-\frac{1}{v_{site}}[\ln(1-\phi) + \phi + \chi\phi^2] + \frac{\phi_0}{N_x v_{site}}\left[\frac{1}{2}\left(\frac{\phi}{\phi_0}\right) - \left(\frac{\phi}{\phi_0}\right)^{1/3}\right] + \left(\sum_{i=0}^{\sigma} c_i^H + \frac{\pi_{ex}^H}{k_B T}\right) - \left(\sum_{i=0}^{\sigma} c_i^B + \frac{\pi_{ex}^B}{k_B T}\right) = 0 \quad (20)$$

where π_{ex}^H and π_{ex}^B are the excess osmotic pressure corrections for the hydrogel and bath phases, respectively. The excess osmotic pressure based on the extended Debye−Hückel limiting law is given by

$$\left(\frac{\pi_{ex}}{k_B T}\right)_{DHLL'} = -\frac{\kappa^3}{24\pi}\left\{\frac{3}{1+\kappa a} - 2\tau(\kappa a)\right\} \quad (21)$$

where the inverse Debye length, κ, and the excluded volume correction, τ, are as previously defined. In the DHLL + B_2 approximation the excess osmotic pressure is

$$\left(\frac{\pi_{ex}}{k_B T}\right)_{DHLL+B_2} = -\frac{5\kappa^3}{192\pi} - \sum_{i=1}^{\sigma}\sum_{j=1}^{\sigma} c_i c_j S_{ij}(\kappa) - \frac{\kappa}{8\pi\epsilon\epsilon_0 k_B T}\sum_{i=1}^{\sigma}\sum_{j=1}^{\sigma} c_i c_j S'_{ij}(\kappa) \quad (22)$$

where S_{ij} is as defined earlier, and

$$S'_{ij}(\kappa) = 2\pi\int_0^\infty \left\{\exp\left[-\frac{u^*_{ij}(r)}{k_B T}\right]\exp(q_{ij}(r)) - 1\right\} \exp(-\kappa r) r^2\, dr \quad (23)$$

As previously discussed, the excess osmotic pressure can also be calculated from integral equation methods and the pressure equation modified to include more than one component: that is,

$$\left(\frac{\pi_{ex}}{k_B T}\right) = -\frac{1}{6}\sum_{i=1}^{\sigma}\sum_{j=1}^{\sigma} c_i c_j \int_0^\infty r\,\frac{\partial u_{ij}(r)}{\partial r}\, g_{ij}(r)(4\pi r^2)\, dr \quad (24)$$

The chemical potential of the ith ionic species in the hydrogel phase is given by the relation

$$\mu^\circ_i + k_B T\ln\left(\frac{N_i}{V}\right) + z_i e\varphi + k_B T\ln\gamma_i = \mu^\circ_i + k_B T\ln\left(\frac{N_i^B}{V^B}\right) + z_i e\varphi^B + k_B T\ln\gamma_i^B \quad (25)$$

where μ°_i and γ_i are the standard state chemical

potential and activity coefficient of the *i*th ion, respectively. This leads to relations between ions *i* and *j* of the form

$$\left(\frac{C_i\gamma_i}{C_i^{\mathrm{B}}\gamma_i^{\mathrm{B}}}\right)^{1/z_i} = \left(\frac{C_j\gamma_j}{C_j^{\mathrm{B}}\gamma_j^{\mathrm{B}}}\right)^{1/z_j} \tag{26}$$

where capital letters are used to represent molar quantities. In the limit of small ion concentrations the activity coefficients approach unity and the familiar Donnan relations,

$$(C_i/C^{\mathrm{B}}{}_i)^{1/z_i} = (C_j/C_j^{\mathrm{B}})^{1/z_j} \tag{27}$$

are recovered.

Equality of chemical potentials between unbound and bound hydrogen ion states can be expressed as

$$\mu^\circ_{\mathrm{A}^-} + k_{\mathrm{B}}T\ln\left(\frac{N_{\mathrm{A}^-}}{V}\right) + z_{\mathrm{A}^-}e\varphi + k_{\mathrm{B}}T\ln\gamma_{\mathrm{A}^-} + \mu^\circ_{\mathrm{H}^+} + k_{\mathrm{B}}T\ln\left(\frac{N_{\mathrm{H}^+}}{V}\right) + z_{\mathrm{H}^+}e\varphi + k_{\mathrm{B}}T\ln\gamma_{\mathrm{H}^+} = \mu^\circ_{\mathrm{AH}} + k_{\mathrm{B}}T\ln\left(\frac{N_{\mathrm{AH}}}{V}\right) + k_{\mathrm{B}}T\ln\gamma_{\mathrm{AH}} \tag{28}$$

where the subscripts A^-, AH, and H^+ refer to the dissociated acidic monomer, the undissociated acidic monomer, and the hydrogen ion, respectively. A similar relation can be written for base dissociation, so the acid and base dissociation constants become

$$K_{\mathrm{a}} = \gamma_{\mathrm{A}^-}C_{\mathrm{A}^-}\gamma_{\mathrm{H}^+}C_{\mathrm{H}^+}/\gamma_{\mathrm{AH}}C_{\mathrm{AH}} \tag{29}$$

$$K_{\mathrm{b}} = \gamma_{\mathrm{BOH}}C_{\mathrm{BOH}}\gamma_{\mathrm{H}^+}C_{\mathrm{H}^+}/\gamma_{\mathrm{B}^+}C_{\mathrm{B}^+} \tag{30}$$

where the subscripts B^+ and BOH refer to the dissociated and undissociated basic monomeric states. At low ion strengths the activity coefficients approach unity and the relations

$$K_{\mathrm{a}} = C_{\mathrm{A}^-}C_{\mathrm{H}^+}/C_{\mathrm{AH}} \tag{31}$$

$$K_{\mathrm{b}} = C_{\mathrm{BOH}}C_{\mathrm{H}^+}/C_{\mathrm{B}^+} \tag{32}$$

are recovered.

The internal ion concentrations and swelling equilibria were determined iteratively using a combination of Newton's method and bisection. The activity coefficients of the ions in the bath phase were determined from the bath ion concentrations, while the ion activity coefficients in the hydrogel phase were initially set to unity. For a given internal hydrogen ion concentration the acid and base dissociation equations and the modified Donnan relations determined all other ion concentrations and hence the total internal net charge. The hydrogen ion concentration that satisfied charge electroneutrality was then determined. From the calculated internal ion concentrations, the internal activity coefficients were recalculated and the process iterated to determine a new set of ion concentrations. Once the ion concentrations had converged, they were used to calculate the osmotic pressure difference between the hydrogel and bath phase. The hydrogel densities that gave rise to zero osmotic pressure differences were then determined. The choice of parameters based on our experimental system is described in a previous paper.[4]

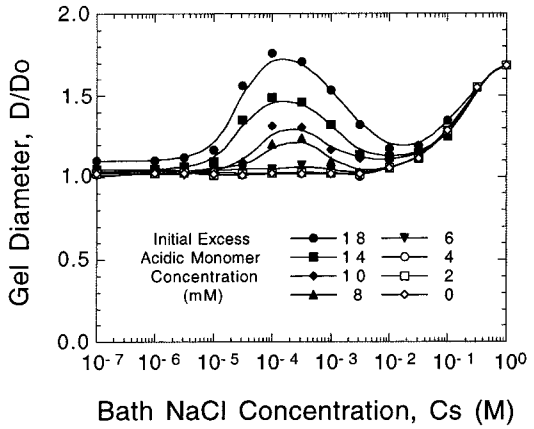

Figure 1. Polyampholyte hydrogel equilibrium swelling relative to the casting diameter (D_0) versus bath salt concentration and initial excess acidic monomer concentration. Polyampholyte swelling increases monotonically with increasing initial excess acidic monomer concentration. The solid lines join the experimental measurements of a given hydrogel, and error estimates are smaller than the data symbols.

Results and Discussion

Figure 1 shows the observed swelling equilibria of polyampholyte hydrogels initially prepared with a total monomer concentration of 1.4 M. The lowest curve in Figure 1 represents the equilibrium swelling of a polyampholyte hydrogel prepared with a balanced concentration of acidic and basic monomers. The progressively higher swelling equilibrium curves were obtained from polyampholytes with an increasing relative concentration of acidic monomers. At low ionic strengths a collapse transition was observed for both balanced and unbalanced polyampholytes. Unbalanced polyampholytes underwent a swelling transition when the bath salt concentration increased from 1 to 100 μM. Between 0.1 and 10 mM unbalanced polyampholytes collapsed. Further increases in the bath salt concentration produced swelling transitions in all hydrogels. The observed swelling pattern as a function of bath salt concentration and excess acidic monomer concentration can be understood by considering physical models with increasing degrees of complexity.

The lowest, or zero, order approximation for the ion osmotic pressure in a Mayer ionic solution theory is equivalent to the Donnan approximation. In the Donnan model a uniform potential background is assumed to exist in both the hydrogel and bath phases. Figure 2 shows the effect of varying the hydrogel charge offset in such a model where the solvent quality and elastic parameters remain constant. As the charge offset increases, the swelling equilibrium at low ionic strengths increases and reaches a maximum value determined by the solvent and elastic forces. The collapse transition of charged hydrogels at intermediate bath salt concentrations is the result of a decreasing osmotic pressure difference between the hydrogel and bath phases. This model is, therefore, only capable of predicting the collapse transition of unbalanced polyampholytes at intermediate bath salt concentrations.

Figure 3 shows the effect of including acid dissociation in the two phase Donnan model where the pK_{a} of the acidic monomers is 1.5 and the reference state or initial monomer concentration is 1.4 M. The collapse transi-

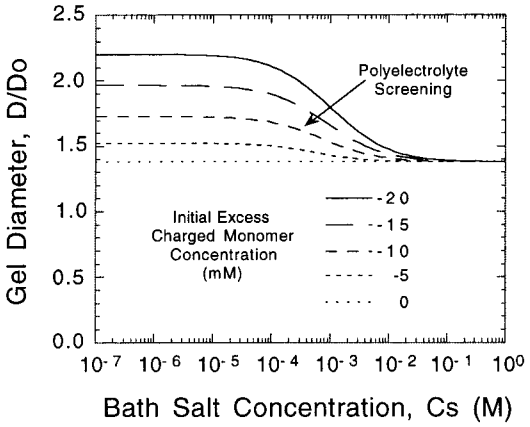

Figure 2. Polyampholyte hydrogel swelling equilibria with varying initial charged monomer concentration predicted by the Donnan approximation. At very low bath ionic strengths the swelling reaches a maximum value determined by the charge, solvent, and elastic forces of the hydrogel. A collapse transition occurs at intermediate bath salt concentrations as a result of a decreasing ion osmotic pressure difference between the hydrogel interior and the surrounding bath.

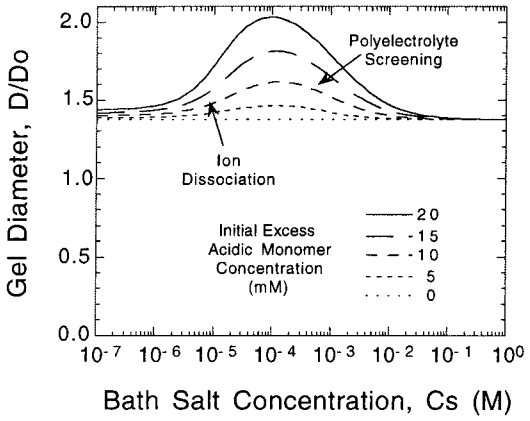

Figure 3. Polyampholyte hydrogel swelling equilibria with varying initial acidic monomer concentration predicted by the Donnan approximation. Including the ion dissociation equilibrium of pK_a = 1.5 acidic monomers leads to a collapse transition at low bath ionic strengths in agreement with the data shown in Figure 1. A polyelectrolyte collapse transition occurs at intermediate bath salt concentrations, but polyampholyte swelling at high ionic strengths is not predicted.

tion at low ionic strengths is the result of hydrogen ion association and is in agreement with the observed swelling transitions shown in Figure 1. The collapse transition of unbalanced polyampholytes with an excess concentration of AMPS−Na at low bath ionic strengths also explains the "aging" effect reported in previous studies.[2] The viscosity of AMPS−Na homopolymer solutions have been observed to decrease over time, particularly when the aqueous solutions are at low ionic strengths. This phenomenon is consistent with the slow exhange of sodium ions for hydrogen ions that occurs at low ionic strengths. This effect is generally overlooked because of the very low pK_a of AMPS−H. Dissolved carbon dioxide and the consequent formation of carbonic acid can make these collapse transitions even more pronounced.[4]

Although Figures 2 and 3 qualitatively explain the effect of ion dissociation and hydrogel charge offset, it is clear that a simple Donnan or uniform potential model does not capture the swelling transitions that occur at higher bath ionic strengths. In Figures 2 and 3 the effect of charge fluctuations that occur on a Debye length scale are completely ignored. It is at this point we must appeal to higher order terms of the Mayer theory to improve our model. As an initial attempt to capture the observed polyampholyte swelling transitions at high bath salt concentrations, one could consider first order correction terms in the Mayer expansion or the equivalent DHLL. Figure 4, however, shows the net ion osmotic pressure predicted by the DHLL for balanced polyampholytes with different fixed concentrations of polyions. At both high polymer and bath salt concentrations the osmotic pressure becomes unphysically high and negative. Considering the range of polymer and bath ion concentrations in this study, the DHLL approximation is unsuitable. The extended DHLL with the excluded volume correction, given by eqs 8 and 9, provides some improvement but still very poor agreement with our experimental results.

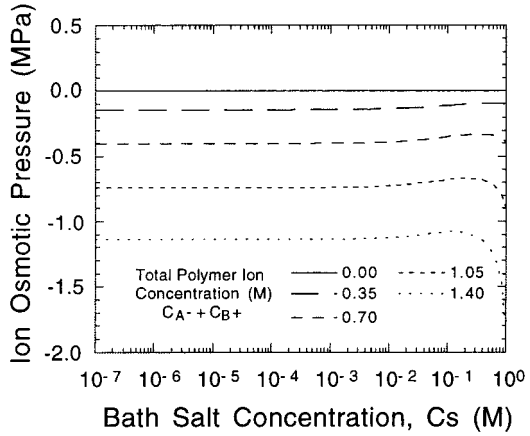

Figure 4. Ion osmotic pressure contributions predicted by the DHLL for fixed concentrations of balanced polymer charges versus bath salt concentration. Attempting to include polyampholyte swelling effects at high ion concentrations with the DHLL leads to unphysically high ion osmotic pressures. Furthermore, a negative contribution to the ion osmotic pressure is predicted at high ion concentrations in contradiction to the data presented in Figure 1.

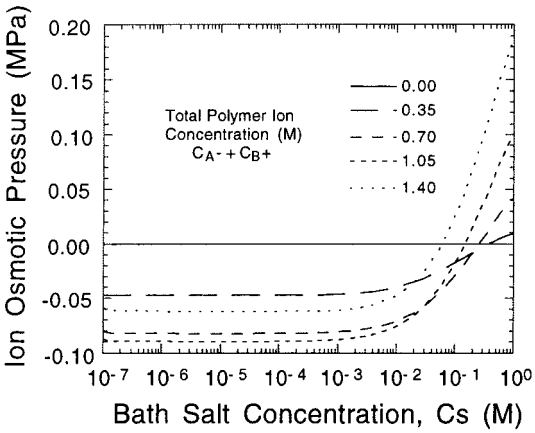

Figure 5. Ion osmotic pressure contributions predicted by the DHLL + B_2 approximation for fixed concentrations of balanced polymer charges versus bath salt concentration. The DHLL + B_2 approximation predicts ion osmotic pressures that are in much better agreement with the observed polyampholyte swelling, particularly at high ion concentrations.

Figure 5 shows the ion osmotic pressures predicted by the DHLL + B_2 approximation arising from different fixed concentrations of balanced positive and negative polyions as a function of bath salt concentration. Com-

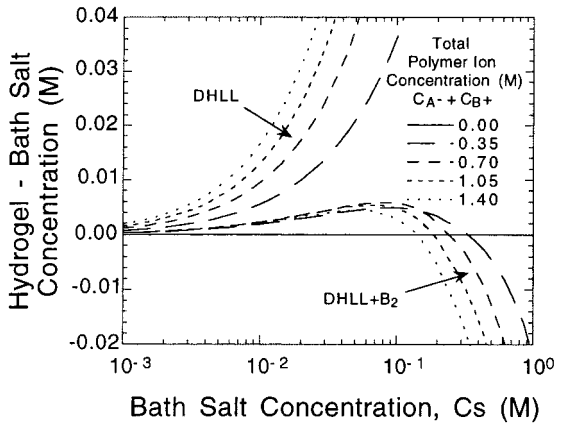

Figure 6. Excess internal ion concentrations in balanced polyampholytes with varying polyion charge densities predicted by the DHLL and the DHLL + B_2 approximations. In both the DHLL and DHLL + B_2 approximations, the internal ion concentration of a balanced polyampholyte is higher inside the hydrogel than in the bath at low ionic strengths. At higher polyion and bath ion concentrations, however, the DHLL + B_2 approximation predicts an exclusion of ions from the hydrogel relative to the bath.

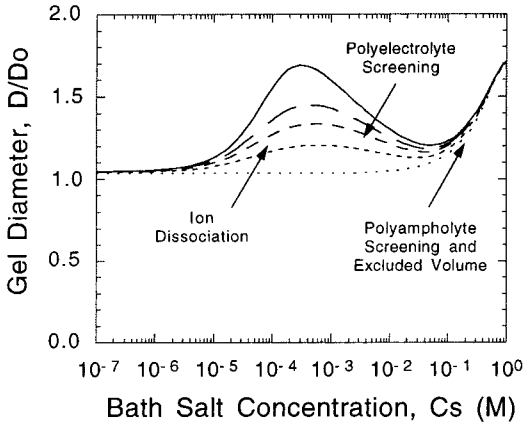

Figure 7. Swelling equilibria predicted by the DHLL + B_2 approximation are in qualitative agreement with the experimental results shown in Figure 1. At low ionic strengths ion dissociation dominates the swelling response of unbalanced polyampholytes. Polyelectrolyte screening occurs at intermediate ionic strengths, and polyampholyte screening occurs at high ionic strengths. At very high ionic strengths repulsive hard core interactions contribute to the swelling forces.

pared to Figure 4, the ion osmotic pressures shown in Figure 5 do not diverge to unphysically large negative values at high ion concentrations but instead give rise to swelling pressures in qualitative agreement with our experimental results. At low bath ion concentrations increasing the polyion charge density results in an increasing polyampholyte attraction until excluded volume effects counteract this with increasing pressures. Polyampholyte swelling transitions at high bath salt concentrations, therefore, include not only electrostatic shielding but hard core excluded volume effects.

Figure 6 shows the difference between the internal and bath salt concentrations in balanced hydrogels with varying fixed total charge concentrations. Like the DHLL approximation, the DHLL + B_2 approximation also predicts a higher internal mobile ion concentration at low bath salt concentrations.[12] At higher bath salt concentrations, however, the internal ion concentration can actually become smaller than the bath concentration. This effect, which is not predicted by the DHLL, is another manifestation of the hard core contribution to the osmotic pressure by both the polyions and mobile ions.

Other approximations that include more terms of the Mayer expansion, such as the PY and HNC approximations, can also be similarly applied. Like the DHLL + B_2 approximation, unphysically large osmotic pressures associated with ignoring the hard core repulsive interactions are overcome. The shortcoming of these methods is their numerical intensity. The $g(\Lambda)$ is particular attractive in this regard since it yields solutions close to the PY and HNC approximations without requiring complicated iterative methods.[17]

Figure 7 shows the effect of simultaneously balancing both the solvent and ion chemical potentials in the DHLL + B_2 approximation with the inclusion of ion dissociation. At very low ion strengths ion dissociation equilibrium dominates the swelling response and gives rise to the swelling transition between 10 and 100 μM bath salt concentrations. Increasing the bath salt concentration causes a shielding of the polyelectrolyte and then polyampholyte swelling forces. Using the DHLL + B_2 approximation gives us a good qualitative agreement with the data shown in Figure 1. Compared to Figure 1, however, the charge offsets required to give the corresponding swelling ratios are higher. Improvements can be made by using a PY or HNC at the expense of greater numerical complexity.

From both the experimental data presented in Figure 1 and the theoretical predictions shown in Figure 7 one notices that polyelectrolyte screening occurs when the bath salt concentration becomes comparable to the excess charge concentration. Notice also that polyampholyte shielding occurs when the bath salt concentration becomes comparable to the polymer ion concentration. An additional effect related to the hard core repulsion of the individual ions becomes important when the Debye length is comparable to the hard core ionic radius. If much greater charge offsets had been chosen relative to the background of balanced polymer charges, the separation of polyelectrolyte and polyampholyte screening effects would not be so clear. In addition, the rodlike configuration that develops when a large linear charge density is present would make the assumption of a polymer ion plasma completely invalid.

A number of future extensions can be made to our model. Similar to the model of Higgs and Joanny,[12] our work treats the electrostatic contributions from polyions as free ions in solution. A more advanced treatment would include the elastic correlation between monomers simultaneously with the ion screening.[23] We have also overlooked contributions from condensation and have assumed the acid and base dissociation constants are similar to those of the monomers in dilute solutions. Despite these limitations, however, our model captures the overall swelling behavior without the unphysical osmotic pressure contributions associated with the DHLL at high ionic strengths.

Conclusions

A sequence of theoretical approximations based on the Mayer ionic solution theory has been used to understand polyampholytic hydrogel swelling transitions over a wide range of bath salt concentrations. The Donnan, or zero order, approximation was successfully applied to interpreting the effects of ion dissociation and polyelectrolyte collapse transitions. An attempt to capture

polyampholyte swelling transitions by applying a first order correction in the form of the DHLL was unsuccessful because of unphysically large osmotic pressures that occur at high ion concentrations in this model. The extended Debye−Hückel model also gave very poor agreement with our data. Much better qualitative agreement was obtained when second order Mayer corrections were included using the DHLL + B_2 approximation. At high bath salt concentrations electrostatic screening and excluded volume effects contributed to the swelling of polyampholytic hydrogels. Further improvements can be made at the expense of greater numerical complexity by implementing the PY and HNC approximations which include more terms in the Mayer expansion.

Acknowledgment. A.E.E. acknowledges fellowship support from Raytheon, Rhône-Poulenc Rorer, the National Science and Engineering Research Council of Canada, and the Medical Research Council of Canada. This work was partially supported by National Science Foundation Grant DMR 90-22933 and by National Institutes of Health Grant GM/HL 49039. E.R.E. thanks the Burroughs-Wellcome Fund in Experimental Therapeutics and the Whitaker Foundation in Biomedical Engineering. We thank Professor S.-H. Chen for useful discussions.

References and Notes

(1) Baker, J. P.; Blanch, H. W.; Prausnitz, J. M. *Polymer* **1995**, *36*, 1061.
(2) Corpart, J.; Candau, F. *Macromolecules* **1993**, *26*, 1333.
(3) Skouri, M.; Munch, J. P.; Candau, S. J.; Neuret, S.; Candau, F. *Macromolecules* **1994**, *27*, 69.
(4) English, A. E.; Mafe, S.; Manzanares, J. A.; Yu, X.; Grosberg, A. Y.; Tanaka, T. *J. Chem. Phys.* **1996**, *104*, 8713.
(5) English, A. E.; Tanaka, T.; Edelman, E. *J. Chem. Phys.* **1996**, *105*, 10606.
(6) Gutin, A. M.; Shakhnovich, E. I. *Phys. Rev. E* **1994**, *50*, R3322.
(7) Kantor, Y.; Kardar, M. *Phys. Rev. E* **1995**, *51*, 1299.
(8) Kantor, Y.; Kardar, M. *Phys. Rev. E* **1995**, *52*, 835.
(9) Wittmer, J.; Johner, A.; Joanny, J. F. *Europhys. Lett.* **1993**, *24*, 263.
(10) Victor, J. M.; Imbert, J. B. *Europhys. Lett.* **1993**, *24*, 189.
(11) Dobrynin, A. V.; Rubinstein, M. *J. Phys. II* **1995**, *5*, 677.
(12) Higgs, P. G.; Joanny, J. *J. Chem. Phys.* **1991**, *94*, 1543.
(13) McMillan, W. G.; Mayer, J. E. *J. Chem. Phys.* **1945**, *13*, 276.
(14) Mayer, J. E. *J. Chem. Phys.* **1950**, *18*, 1426.
(15) Allnatt, A. R. *Mol. Phys.* **1964**, *8*, 533.
(16) Rasaiah, J. C. *J. Chem. Phys.* **1970**, *52*, 704.
(17) Rasaiah, J. C.; Friedman, H. L. *J. Chem. Phys.* **1968**, *48*, 2742.
(18) Rossky, P. J.; Dale, W. D. T. *J. Chem. Phys.* **1980**, *73*, 2457.
(19) English, A. E.; Tanaka, T.; Edelman, E. R. *J. Chem. Phys.* **1997**, *107*, 1645.
(20) Debye, P. W.; Hückel, E. *Phys. Z.* **1923**, *24*, 185.
(21) McQuarrie, D. A. *Statistical Mechanics*; Harper and Row: New York, 1976.
(22) Meeron, E. *J. Chem. Phys.* **1957**, *26*, 804.
(23) Borue, V. Y.; Erukhimovich, I. Y. *Macromolecules* **1988**, *21*, 3240.

MA971207O